



UPPSALA
UNIVERSITET

*Digital Comprehensive Summaries of Uppsala Dissertations
from the Faculty of Pharmacy 304*

A pharmacokinetic approach to intra-brain distribution with a focus on cyclic peptides

ERIK MELANDER



ACTA
UNIVERSITATIS
UPSALIENSIS
UPPSALA
2022

ISSN 1651-6192
ISBN 978-91-513-1364-1
URN urn:nbn:se:uu:diva-460177

Dissertation presented at Uppsala University to be publicly examined in B42, Biomedicinskt Centrum (BMC), Husargatan 3, Uppsala, Friday, 11 February 2022 at 09:15 for the degree of Doctor of Philosophy (Faculty of Pharmacy). The examination will be conducted in English. Faculty examiner: Xavier Declèves (Université de Paris, France).

Abstract

Melander, E. 2022. *A pharmacokinetic approach to intra-brain distribution with a focus on cyclic peptides*. *Digital Comprehensive Summaries of Uppsala Dissertations from the Faculty of Pharmacy* 304. 49 pp. Uppsala: Acta Universitatis Upsaliensis. ISBN 978-91-513-1364-1.

When designing treatments for disorders of the central nervous system (CNS) reaching the site of action is a major hurdle in the development process. Regardless if the target is extra- or intracellular, precise measurements to understand the distribution within the CNS are required. There is however a lack of understanding of differences in blood-brain barrier transport and intra-brain distribution of both small and large molecules. In this thesis the regional Blood-Brain Barrier transport of antipsychotic agents, along with their brain tissue binding and regional cellular accumulation was quantified. Furthermore, a novel LC-MS/MS method was developed for the quantitative analysis of the cyclic peptide kalata B1 was developed for analysis of brain tissue and plasma samples. The Blood-Brain Barrier transport, permeability, intra-brain distribution and cellular accumulation were assessed for two cyclic peptides, SFTI-1 and kalata B1.

The antipsychotics exhibited clear differences in their regional BBB transport as well as their brain tissue binding, with the most dramatic spatial differences in BBB transport being observed for the p-glycoprotein substrates risperidone and paliperidone. The highest level of transporter mediated protection was observed in the cerebellum, with pronounced efflux for several of the antipsychotics. The development of a quantitative method for the cyclic peptide kalata B1 was successfully validated and applied to measure low concentration of the peptide in biological matrices. The BBB transport of SFTI-1 was markedly higher than that of kalata B1 whereas both peptides exhibited similar permeability across an in vitro BBB model. It was also shown that SFTI-1 resides mainly within the interstitial fluid within the brain, but that kalata B1 readily enters the cells of the brain parenchyma. The cellular accumulation of kalata B1 was abolished under cold conditions, and was not observable in lung tissue, suggesting an active process that is tissue specific. It was also shown that both peptides are taken up into cell cultures of neurons and astrocytes.

In conclusion this thesis and the studies herein contribute to a better understanding of distribution patterns of both antipsychotics and cyclic peptides and provides valuable lessons in terms of what types of studies should be prioritized for the development of such molecules into therapeutic agents.

Erik Melander, Department of Pharmacy, Box 580, Uppsala University, SE-75123 Uppsala, Sweden.

© Erik Melander 2022

ISSN 1651-6192

ISBN 978-91-513-1364-1

URN urn:nbn:se:uu:diva-460177 (<http://urn.kb.se/resolve?urn=urn:nbn:se:uu:diva-460177>)

To my family

List of Papers

This thesis is based on the following papers, which are referred to in the text by their Roman numerals.

- I. Loryan I, Melander E, Svensson M, Payan M, König F, Jansson B och Hammarlund-Udenaes M. **In-depth neuropharmacokinetic analysis of antipsychotics based on a novel approach to estimate unbound target-site concentration in CNS regions: link to spatial receptor occupancy.** *Mol Psychiatry* 2016 Nov;21(11):1527-1536. doi: 10.1038/mp.2015.229.
- II. Melander E, Eriksson C, Jansson B, Göransson U, Hammarlund-Udenaes M. **Improved method for quantitative analysis of the cyclotide kalata B1 in plasma and brain homogenate.** *Biopolymers*. 2016 Nov;106(6):910-916. doi: 10.1002/bip.22984.
- III. Melander E, Eriksson C, Wellens S, Culot M, Göransson U, Loryan I, Hammarlund-Udenaes M. **Dual behavior of cyclic peptides at the blood-brain barrier vs brain cellular uptake: Importance for CNS drug development.** 2021. *In Manuscript*
- IV. Melander E, Hosseini K, Eriksson C, Fredriksson R, Göransson U, Hammarlund-Udenaes M, Loryan I. **Cellular uptake and intra-brain distribution of cyclic cell penetrating peptides: why tissue and cell type matters.** 2021. *In Manuscript*

Reprints were made with permission from the respective publishers.

Contents

Introduction.....	11
The Blood-brain Barrier	12
Regional differences in Blood-Brain Barrier properties	13
BBB transport	14
Pharmacokinetic concepts in BBB transport	14
Intra-brain distribution	16
Cellular uptake and distribution pathways.....	17
Cell penetrating peptides	18
Cyclic cell penetrating peptides.....	19
Aims.....	20
Materials and Methods.....	21
Animals	21
Peptide production.....	21
Experimental procedures	22
In vivo pharmacokinetics.....	22
Blood-brain barrier transport	22
In vitro blood-brain barrier permeability	23
In vitro binding assay.....	23
In vitro unbound tissue volume of distribution assay	24
Cellular accumulation assay	26
Bioanalytical setup	27
Results & Discussion	29
Regional distribution of antipsychotics (Paper I)	29
Validation of bioanalytical method for kalata B1 (Paper II)	32
Blood-Brain Barrier transport of cyclic peptides (Paper III).....	33
In vivo Blood-Brain Barrier transport	33
In vitro Blood-Brain Barrier permeability	36
Intra brain distribution and cellular uptake of cyclic peptides (Paper IV)	37
Cellular uptake of SFTI-1 and kalata B1	38
Conclusions.....	40
Acknowledgements	42
References.....	43

Abbreviations

ABC	ATP-binding cassette
ACN	Acetonitrile
AUC _{brain}	Area under the brain concentration-time curve
AUC _{plasma}	Area under the plasma concentration-time curve
BBB	Blood-Brain Barrier
BCRP	Breast Cancer Resistance Protein
BS	Brain stem
CNS	Central Nervous System
CL	Clearance
CL _{in}	Net influx clearance into the brain
CL _{out}	Net efflux clearance from the brain
CPP	Cell Penetrating Peptide
CRB	Cerebellum
CRT	Cortex
CSF	Cerebrospinal Fluid
ECF	Extracellular Fluid
HPC	Hippocampus
HPT	Hypothalamus
ISF	Interstitial Fluid
K _{p,brain}	Total brain-to-plasma concentration ratio
K _{p,uu,brain}	Unbound brain-to-plasma concentration ratio
K _{p,uu,cell}	Unbound intracellular-to-extracellular concentration ratio
MPA	Mobile Phase A
MPB	Mobile Phase B
P _{app}	Apparent Permeability
PBS	Phosphate Buffered Saline
P _e	Endothelial Permeability
PD	Pharmacodynamics
PK	Pharmacokinetics
PKPD	Pharmacokinetics-Pharmacodynamics
Pgp	P-glycoprotein
SC	Spinal Cord
SD	Standard deviation
SFTI-1	Sunflower Trypsin Inhibitor 1
SLC	Solute Carrier

STR	Striatum
$t^{1/2}$	Half-life
$V_{u,brain}$	Unbound volume of distribution in brain
$V_{u,lung}$	Unbound volume of distribution in lung

Introduction

When designing treatments for disorders of the central nervous system (CNS) reaching the site of action is a major hurdle in the development process. Regardless if the target is extra- or intracellular, precise measurements to understand the distribution within the CNS are required. There is however a lack of understanding of Blood-brain Barrier (BBB) transport and intra-brain distribution of both small and large molecules. A clear example of when this knowledge is essential is in the treatment with antipsychotic agents. These drugs need to reach sufficient receptor occupancy in specific regions of the brain to elicit their effect, whilst distribution to other regions is often responsible for adverse events. By better understanding the distribution patterns of antipsychotic drugs, better treatments can be designed, leading to more successful treatment. Another area where knowledge of intrabrain distribution is highly relevant is the emerging field of cell penetrating peptides (CPPs). These peptides are being seen as a promising alternative for delivery to the CNS, with their cell penetrating capabilities seen as a tool to overcome both the BBB and the cellular barriers within the CNS. In order to establish the feasibility of cell penetrating peptides, their capacity of uptake into the specific cells that they are targeting is needed. So far, studies on CPPs have mainly studied their uptake into peripheral cell types, and extrapolated that uptake to other cell types. Alternatively the uptake into the CNS has been assessed through non-quantitative methods, where the unbound concentrations at the site of action are not properly determined. Such studies have their value, but will not provide sufficient information for proper decision making regarding their usefulness in the treatment of CNS disorders. Amongst the CPPs is a subclass of cyclic cell penetrating peptides, which are more stable than their linear counterparts, and have been postulated to have advantageous properties for intracellular delivery. In both these cases, regardless of whether we are studying the small molecular drugs intended for the treatment of psychotic disorders, or the larger cyclic cell penetrating peptides, proper translation between cell cultures, tissues, and model species are needed in order to inform further development in humans.

The Blood-brain Barrier

The brain, and the spinal cord, as constituents of the central nervous system are organs with a highly regulated microenvironment. This regulation is primarily performed through the function of barriers surrounding the CNS [1,2]. The BBB is a physiological and metabolic barrier separating the brain parenchyma from the systemic circulation. It is comprised of the capillary endothelial cells connected with tight junction proteins, effectively keeping molecules out of the brain. These connections between the endothelial cells are built up of various junction proteins, both tight junctions and adherens junctions [3–5]. Typically these junctions are built up by proteins such as occludin and claudin. This junctional system provides the primary barrier function for both macromolecules and polar solutes, as they are generally prevented from transcellular diffusion. The BBB is part of a wider network of cells in the CNS referred to as the neurovascular unit (Figure 1). This unit consists of the capillary endothelium, as well as other cell types such as pericytes, astrocytes, microglia, and the neurons themselves. The interplay between these cells is crucial for the functioning of the BBB as it involves a multitude of signalling pathways.

The capillary network in the brain is extensive, with a surface area of around 20 m² in total [6]. The BBB is a highly dynamic unit involved in many processes, including the maintenance of brain homeostasis, uptake of nutrients, removal of waste products and the protection of the brain from potentially toxic compounds. The BBB ensures that the concentration of ions in the brain is kept at a correct level, with ion channels controlling the exact concentrations of potassium, sodium, calcium and other ions [7]. Another function of the BBB is the homeostasis of neurotransmitters, where for example the levels of glutamate in blood rise with food intake, but if the BBB didn't restrict its entry, severe harm would be caused to the CNS [8,9]. The BBB is also vital in preventing proteins and other large molecules from entering the brain. Common plasma proteins such as albumin are toxic to the CNS tissue, and these are effectively kept out of the brain and the cerebrospinal fluid (CSF) [10–12]. This also means that the CNS is an immune privileged site, where neutrophil infiltration is low, and immune cells have limited access to the brain parenchyma, except post trauma or ischemia or related inflammations [13].

All of these barrier functions pose a problem for drug development, since the BBB is equipped with various transporters that prevent several therapeutic agents from entering the brain in sufficient concentrations to elicit their effect. The BBB is not the only barrier within the CNS though. There is also the blood-cerebrospinal fluid-barrier, separating the blood circulation from the CSF which is composed of epithelial cells in the choroid plexus and provides an interface between the CSF and the systemic circulation in which many transporters can be found [14,15].

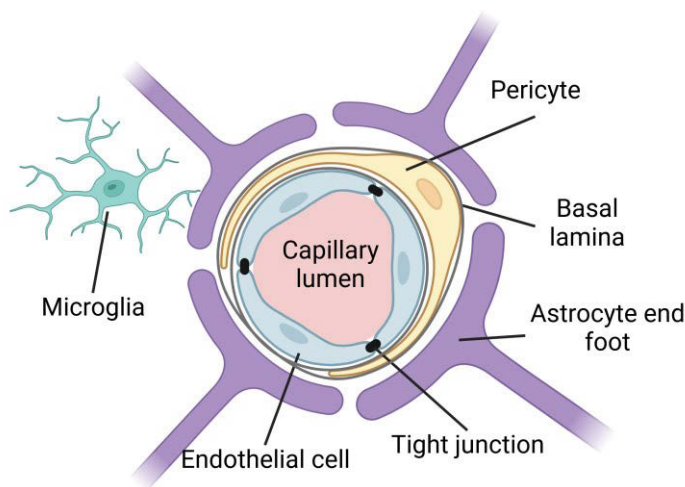


Figure 1. Schematic view of the blood-brain barrier and the wider neurovascular unit with pericytes, astrocytes, and microglia. Created with Biorender.

Regional differences in Blood-brain Barrier properties

When developing a therapeutic agent for a CNS disease or disorder, it is often a specific region of the brain that is targeted, to achieve an effect on certain receptors in that region of the brain. For example, antipsychotic drugs target dopamine D_2 receptors in the mesocortical and mesolimbic regions of the brain. On the other hand, certain adverse events can be connected to the drug eliciting an effect to the same type of receptor in a different region of the brain, such as the dyskinesia that can appear through interaction with D_2 receptors in the striatal area of the brain [16,17]. The antipsychotic drugs also interact with cortical 5-HT_{2A} receptors, and understanding the differential distribution of these drugs can help in calculating their receptor occupancy in the specific area. Examples of these antipsychotic drugs are haloperidol, clozapine, olanzapine, quetiapine, risperidone, and paliperidone. By understanding the regional pharmacokinetic-pharmacodynamic relationship for these compounds, it is possible to better elucidate their effect and side-effect profiles to design better treatments.

It is therefore of interest to understand if there are regional differences in the BBB transport of drugs, and also if there are regional differences in drug tissue binding. Regional differences in the BBB might be explained by differential expression of transporters in different regions of the brain microvasculature. Another, but less likely difference might be that the tight junc-

tions in the BBB are different in different regions, leading to various levels of leakiness through the endothelium.

BBB transport

There are several routes through which a compound can cross from the systemic circulation into the brain parenchyma. Small typically lipophilic compounds can cross the BBB through passive diffusion by a transcellular route through the endothelial cells [18]. This diffusion is only driven by the concentration gradient from blood to brain without any need for energy consumption. In other tissues, paracellular diffusion can also occur, but this pathway is highly restricted at the BBB due to the tight junctions connecting the endothelial cells. Another pathway, of high importance for the transport across the BBB, is carrier mediated transport. This pathway is of importance, not only for the transport of drugs, but also for essential nutrients such as glucose and amino acids into the brain. Carrier mediated transport is also essential for the protective qualities of the BBB, with various transporters hindering the entrance of exogenous compounds into the brain. This pathway functions through transport proteins located in the membrane of the endothelial cells, with some on the luminal side of the endothelium and others on the abluminal side. The most common and well-studied of these transport proteins belong to two families of transporters; ATP-binding cassette- (ABC) and Solute Carrier (SLC) transporters [19]. Within the ABC transporter family we can find important transporters such as P-glycoprotein (Pgp) and breast cancer resistance protein (BCRP). These are responsible for the efflux of a large portion of drugs at the BBB and do therefore pose a large obstacle in the development of effective therapeutics for CNS disorders.

Pharmacokinetic concepts in BBB transport

For the evaluation of transport of drugs into the brain two broad processes are crucial; the rate of transport across the BBB, and the extent of transport across the BBB [18]. The rate of transport into the brain is often described as the permeability of a compound across the BBB, and can either be measured in vivo by methods such as in situ brain perfusion, or in vitro by cell culture transwell studies [20–23]. This phenomenon can be described by several different parameters, such as the permeability surface area product, also called endothelial permeability, CL_{in} , or K_{in} . Permeability determined from in vitro studies is often described with the parameter apparent permeability (P_{app}), but can also be described as the endothelial permeability (P_e). These parameters describe the permeability across the cells and the transwell insert (P_{app}) or only across the cell layer (P_e). The advantage of calculating P_e is that the ability of the studied compound to permeate the insert itself can be a rate limiting step, and by correcting the permeability for this step we can

obtain a clearer picture of the actual permeability across the cells themselves. When performing studies on BBB permeability with in vitro systems it is important to consider the unique properties of the BBB. The cell layer should consist of brain endothelial cells, and if possible the system should include a co-culture with other cells from the neurovascular unit such as pericytes or astrocytes. It has been shown that such a co-culture better promotes the correct BBB phenotype in the model system [21,22,24].

Processes related to the transport of compounds out of the brain, through passive or active transport can be described as a measurement of the clearance out of the brain with the parameter CL_{out} . Whilst the rate of transport can be useful for the understanding of how different uptake processes work, in a clinical setting it is only really useful when discussing acute treatment, where the initial onset of the effect is crucial. With more chronic treatments, it is rather the extent of transport which is the more crucial process. The extent of transport informs us of the ratio of drug that enters the brain relative to that in plasma. It is most clearly described as the unbound brain-to-unbound plasma concentration ratio, $K_{p,uu,brain}$, at steady state conditions, or as unbound brain-to-plasma exposure ratio [18,25].

$$K_{p,uu,brain} = \frac{C_{u,brain}}{C_{u,plasma}} = \frac{AUC_{u,brain}}{AUC_{u,plasma}} \quad \text{Eq 1}$$

In this equation, $C_{u,brain}$ is the unbound concentration in brain tissue and $C_{u,plasma}$ is the unbound concentration in plasma. $AUC_{u,brain}$ is the unbound exposure in brain and $AUC_{u,plasma}$ is the unbound exposure in plasma. The reason for using unbound concentrations is that under the free drug hypothesis, only the unbound drug can cross membranes or elicit an effect on the target receptor [26,27]. It is thus most relevant to measure the unbound concentration whenever possible. This unbound concentration ratio can give us good estimations of the transport processes at the BBB, where a $K_{p,uu,brain} < 1$ indicates net efflux out of the BBB whereas a $K_{p,uu,brain} > 1$ indicates net influx at the BBB. If the $K_{p,uu}$ value is close to unity, this often reflects a compound which mainly crosses the BBB through passive diffusion, though the possibility of both influx and efflux of the same magnitude cannot be excluded.

The direct measurement of unbound concentrations in the brain is typically performed by microdialysis, a technique where a probe is inserted into the tissue, and unbound concentrations are sampled. This method is however not always feasible and other methods are required to access the unbound concentrations in brain and plasma. One such method is the Combinatory Mapping Approach (CMA), which combines in vivo and in vitro methods to calculate $K_{p,uu,brain}$ [28]. Here the total concentrations in brain and plasma are measured through in vivo experiments, providing the total brain-to-plasma ratio, $K_{p,brain}$, which is a composite parameter that describes both the BBB transport as well as the binding characteristics of the compound in both brain

and plasma. To separate the BBB transport from the binding, the $K_{p,brain}$ value is then combined with in vitro assessments of the binding of the compound to both plasma proteins and brain tissue (Figure 2). The most classic way of estimating the binding is via equilibrium dialysis, however, for the assessment of binding in the brain, the more sophisticated brain slice method should be preferred since it can capture more processes than simply the non-specific binding [27,29–31].

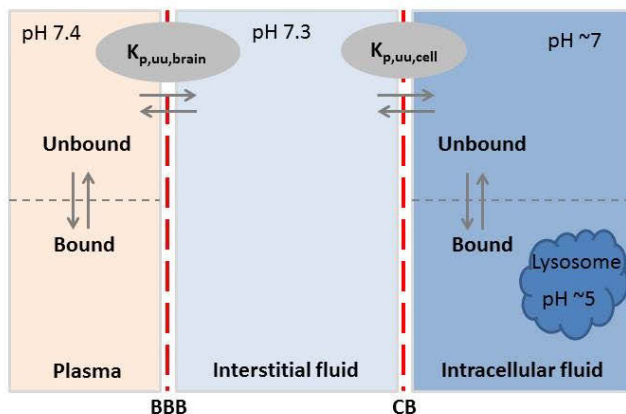


Figure 2. Schematic view over the compartments of the brain and plasma with the BBB and the cellular barrier (CB) are indicated with dashed red lines. Binding equilibria in plasma and brain cells are indicated.

Intra-brain distribution

A separate but also important aspect of the pharmacokinetics within the CNS is the intra-brain distribution of the studied compound. This describes the binding of the compound to the brain tissue, differential distribution between the regions of the brain, and the uptake into cells or subcellular compartments. One of the main parameters that describes the intra brain distribution is $V_{u,brain}$, i.e the unbound volume of distribution of the compound in the brain [31]. This parameter tells us about both specific and non-specific binding in the brain, as well as any cellular uptake, driven either by active processes or by phenomena such as lysosomal trapping, driven by pH differences [32]. Measuring $V_{u,brain}$ is commonly done via the brain slice method, in which thin slices of brains are incubated in artificial extracellular fluid spiked with the studied compound [31]. If no accumulation into the cells of the brain parenchyma occurs, the value of $V_{u,brain}$ inversed should correspond with the value of $f_{u,brain}$, describing the non-specific binding to the brain tissue components. A $V_{u,brain}$ value of 0.2 mL/g brain indicates that the studied compound does not enter the cells of the brain at all, but rather stays in the

interstitial fluid. No upper limit for $V_{u,brain}$ exists, and values above 1000 mL/g brain have been observed [30].

By combining $V_{u,brain}$ and $f_{u,brain}$ we can calculate the parameter $K_{p,uu,cell}$, describing any potential accumulation into cells [32]. A $K_{p,uu,cell}$ value > 1 means that the compound is either actively taken up into the cells, or that it is accumulating by some other means. Examples of this are lysosomal trapping, whereby the pH difference between the cytosol and the lysosome changes the charge of the molecule, causing it to be trapped within the lysosome. Since ionised molecules are incapable of diffusing through membranes, therefore, mainly bases are prone to lysosomal trapping.

Cellular uptake and distribution pathways

Once a compound has entered the brain, there are several pathways by which it may distribute within the brain or be taken up by different cell types. This distribution can either take place via passive diffusion, direct translocation mechanisms, or via energy dependent active uptake (Figure 3). Distribution can also be driven by binding to membranes or cellular components. Since many targets for drugs are found within cells, it is highly important to study this intra-brain distribution, both with regards to cell penetration and accumulation, as well as binding characteristics. When exploring the pathways that may lead to accumulation of the studied compound within cells, i.e. those with a $K_{p,uu,cell}$ value above unity, two main pathways should be considered; active transport through one or several of many transporters present on cell membranes or vesicular uptake through the formation of endocytotic vesicles in the cell membranes [1]. These endocytotic pathways are generally divided into clathrin- and caveolae-mediated endocytosis, which are both dependent on dynamin, a protein that is crucial for the budding of the vesicles from the cell membrane [33,34]. These endocytotic processes are initiated either by a molecule binding to a specific receptor on the cell surface, or by adsorption of the molecule to the cell surface [35]. Examples of such receptor mediated endocytotic systems are the transferrin, insulin and low density lipoprotein receptors. The transferrin receptor system has been studied extensively and several studies have reported success in targeting the transferrin receptor for delivery of large molecules such as antibodies [36,37].

Small molecules are more likely to accumulate in cells through transporter mediated uptake, whereas larger molecules such as peptides and proteins are more likely taken up through vesicular pathways. A third pathway which has been proposed as a pathway for entry into cells for cell penetrating peptides in particular, is the formation of transient pores in the cell membrane [38]. These pores can be formed by the peptides oligomerizing within the cell membrane, thereby forming an opening through which entry can occur, so called Barrel-Stave pores [39]. Another type of pore formation

is that of toroidal pores, where the interaction between the peptide and the cell membrane causes the membrane to fold in on itself, thus forming a pore [40–42]. All in all, these various pathways for cellular entry leads to a multitude of possibilities for molecules, small and large, to enter into the cells of the CNS to elicit their effect.

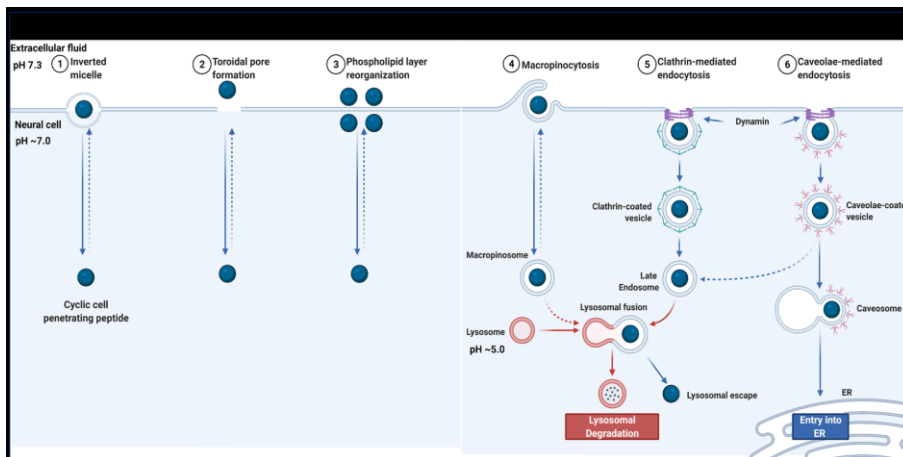


Figure 3. Transcellular uptake pathways for large molecules. The two pathways on the left, clathrin- and caveolae-mediated endocytosis are dynamin dependent. Created with Biorender.

Cell penetrating peptides

A method of overcoming the cellular barrier to deliver therapeutic moieties to intracellular targets could be the use of so called cell penetrating peptides. These first came into the spotlight when the transactivating transcriptional factor (TAT) peptide from the HIV virus was discovered in 1988 [43,44]. TAT is a protein with a high capacity to penetrate cell membranes and enter into the cell. Later, the protein penetratin was also discovered, and together, these discoveries laid the foundation for the development of cell penetrating peptides as system for intracellular delivery [45]. A definition of cell penetrating peptides has been given as a peptide that contains less than 40 amino acids and is able to enter cells by various mechanisms [39]. The amino acid sequence of CPPs varies considerably, but common features are often positively charged amino acids in the sequence. One of the simplest and most used CPPs is just a chain of arginines [39]. It has also been shown that the secondary structure of the peptide can influence the capacity to penetrate into cells. In general, CPPs are not considered to target specific cells, but are assumed to enter cells non-selectively, but certain peptide sequences have

been described to target tissues more specifically, with one example being able to target breast cancer cells [46].

Cell penetrating peptides are generally entering cells through one of the pathways mentioned above, with the most prominent ones being direct penetration of the plasma membrane, or through some form of endocytosis. It should however be noted that the exact mechanisms behind cell penetrating properties of peptides have not yet been fully understood., There are many contradictory reports on uptake mechanisms, and it is likely that the mechanisms might vary depending on experimental conditions, where factors such as pH, cell type, incubation time, and concentration of the peptide can yield different uptake mechanisms in different experiments [47–53]. This is then further proof that in order to properly evaluate the usefulness of a CPP it needs to be studied in the correct system, with conditions matching those of its intended use, i.e as close as possible to physiological conditions, with clinically relevant concentrations if such are known.

Cyclic cell penetrating peptides

One specific subgroup of CPPs is cyclic cell penetrating peptides, which are peptides that have some form cyclic nature, either head-to-tail, head-to-side chain, or side chain-to-side chain [54,55]. They are typically more stable than linear peptides, as the cyclic nature prevents proteolytic degradation. Several cyclic peptides have successfully been developed into medicines, such as cyclosporine A, vancomycin, and daptomycin, and the interest in utilising cyclic peptides to target intracellular targets is increasing [56]. Where larger peptides have issues crossing cellular membranes due to their size and charge of side chains, certain cyclic CPPs are assumed to have a better chance of entering cells due to various transport mechanisms mentioned earlier. Cyclic CPPs are generally considered to enter cells through one of two pathways; either by endosomal uptake or through a direct translocation over the cellular membrane directly into the cytoplasm [54]. A specific group of cyclic CPPs called cyclotides are of particular interest due to their high stability [57–60]. These peptides are of plant origin, have a head-to-tail cyclic structure, and are further stabilized by disulphide bonds between cysteine groups in the peptides. Cyclotides such as kalata B1 and MCoTI have been reported to be able to penetrate into cells [41,61]. Furthermore the plant derived cyclic peptide sunflower trypsin inhibitor (SFTI-1), which shares many characteristics with the cyclotides but is smaller in size, 15 amino acids vs the 28 amino acids found in kalata B1, has also been reported to have cell penetrating potential [62].

Aims

The overall aim of this thesis was to further develop a pharmacokinetic framework for quantifying regional differences in blood-brain barrier transport, and intra-brain distribution of small molecules and cell penetrating peptides.

The specific aims were the following:

1. To investigate possible regional distribution of drugs in the CNS with antipsychotics as model drugs
2. To build a basis for studies of cyclic peptides and their behavior at the BBB and in the brain, by developing a quantitative LC-MS/MS method for the analysis of biological samples of the cyclic peptide kalata B1
3. To investigate in vivo, ex vivo and in vitro BBB transport and intra-brain distribution properties of the model cyclic peptides kalata B1 and SFTI-1, to increase the knowledge about their possible use as scaffolds for CNS drug delivery
4. To evaluate the intra-brain distribution of the cyclic peptides kalata B1 and SFTI-1 in tissues ex vivo in comparison to cells in culture to further investigate distribution patterns

Materials and Methods

Animals

Male Sprague-Dawley rats (250-300 g) were used in all experiments (Taconic, Lille Skensved, Denmark). All animal experiments were performed in accordance with the guidelines from the Swedish National Board for Laboratory Animals, and were approved by the Animal Ethics Committee of Uppsala, Sweden approval numbers: C16/12, C351/11, C188/14. The animals were housed in groups with *ad libitum* access to food and water and with a 12 hour light-dark cycle, and were allowed to rest for 7 days before the study start.

For in vivo pharmacokinetic and neuropharmacokinetic experiments in papers I, II, and III, catheters made of polyethylene (PE50) were implanted in the femoral veins and arteries of the animals for dosing and sampling. All surgeries were performed the day before the experiments under isoflurane anaesthesia. During the experiments the animals were housed in a CMA120 system (CMA, Solna, Sweden) allowing for free movement and *ad libitum* access to food and water.

Peptide production

SFTI-1 was extracted as follows: seeds from *Helianthus annuus*, common sunflower, were crushed and extracted with 60 % AcN for 3 h. The mixture was filtered and the seeds were re-extracted in fresh solvent for an additional 3 h. Following filtration, the extracts were pooled and the major part of AcN was removed by rotary evaporation. The extract was separated from lipids through partitioning against dichloromethane (1:2, v/v). The aqueous layer was freeze-dried, dissolved in MQ-water with 10 % AcN and 0.05 % TFA, and subjected to solid phase extraction on a C18 Isolute™ cartridge (Biotage, Uppsala, Sweden). The extract was loaded, washed with 0.05 % TFA in MilliQ-water and eluted with increasing concentrations of AcN in MilliQ-water with 0.05 % TFA. The SFTI-1 containing fractions were pooled, diluted and purified on Reverse Phase-HPLC (C18, 250 x 10 mm, 5 µm, 300 Å, Phenomenex, Torrance, CA, USA). Purity and identity of SFTI-1 were analysed by HPLC-UV (Shimadzu, Tokyo, Japan) and UPLC-MS/MS (Waters, Milford, MA).

Kalata B1 was extracted and purified from the leaves of *Oldenlandia affinis* with the same procedure as SFTI-1 using a similar protocol [63]. The plant material was homogenized and extracted with dichloromethane/methanol (1:1, v/v). The extract was then freeze dried and then dissolved in 10 % methanol in water and separated on a C18 column. The peptide containing fraction was purified and analysed with LC-MS. Both peptides were > 95 % pure.

Experimental procedures

In vivo pharmacokinetics

In Papers II and III the in vivo pharmacokinetics of SFTI-1 and kalata B1 were assessed, since the information on the PK of cyclic peptides was very limited. Both peptides were given at a dose of 1 mg/kg body weight to healthy male Sprague-Dawley rats. The dose was administered as a 10 min short infusion after which plasma samples were taken for two hours for SFTI-1 and four hours for kalata B1. All samples were added to heparinized low binding Eppendorf tubes. They were then centrifuged and the plasma was transferred to new tubes and frozen. The samples were analysed and the concentration-time curves were used to determine pharmacokinetic parameters such as half-life, clearance, and volume of distribution with non-compartmental methods.

Blood-brain barrier transport

In Papers I and III the BBB transport was assayed by measurement of the parameters $K_{p,brain}$ and $K_{p,uu,brain}$. These were obtained from steady state measurements of brain and plasma concentrations after a 4 hours constant rate infusion. Plasma samples were taken repeatedly during the infusion to ensure that steady state conditions were obtained and maintained. After the infusion, a heart puncture was performed and the whole brain was collected. In Paper I the brain was then further dissected into the regions of interest; hypothalamus, cerebellum, frontal cortex, striatum, hippocampus, and brainstem. The spinal cord was also collected. All tissue and plasma samples were immediately frozen on dry ice and stored pending analysis. To calculate $K_{p,brain}$ and $K_{p,uu,brain}$ the following equations were used:

$$K_{p,brain} = \frac{C_{brain}}{C_{plasma}} \quad (\text{Eq. 2})$$

$$K_{p,uu,brain} = \frac{K_{p,brain}}{f_{u,plasma} * V_{u,brain}} \quad (\text{Eq. 3})$$

The calculation of $K_{p,uu,brain}$ was performed using the CMA, either for whole brain, or for the brain region of interest [28]. This methodology utilises a combination of in vivo and in vitro methods where both BBB transport and binding and distribution characteristics of the studied compound are assessed in order to provide the full picture of the extent of the BBB transport.

In vitro blood-brain barrier permeability

In order to measure the permeability of the two peptides, SFTI-1 and kalata B1, an in vitro BBB model was used. The model was based on CD34+ endothelial cells derived from human hematopoietic stem cells in co-culture with bovine brain pericytes [21,22]. The experiment was set up in a transwell system, and incubated for three hours after which the concentrations in both the donor and receiver compartments were measured. The concentration of peptide was also measured in the endothelial cells themselves, to understand if any fraction of the added peptide was able to enter into the endothelium without crossing to the receiver compartment. From these studies, the permeability parameters P_e and P_{app} were calculated.

$$\frac{1}{P_{se}} = \frac{1}{P_{st}} - \frac{1}{P_{sf}} \quad (\text{Eq 4})$$

$$P_e = \frac{P_{se}}{S} \quad (\text{Eq 5})$$

$$P_{app} = \frac{J}{S \cdot C_0} \quad (\text{Eq 6})$$

Where P_{se} is the permeability surface area product across the endothelial cell layer, P_{st} is the total permeability surface area product across the endothelial cell layer and filter insert, and P_{sf} is the permeability surface area product across the filter insert. S is the surface area of the transwell insert (in this experiment 1.12 cm²). P_{app} is the apparent permeability, J is the rate of appearance of the compound in the receiver compartment (amount/sec), and C_0 is the concentration in the donor compartment at the start of the experiment.

To ensure the integrity of the endothelial monolayer, sodium fluorescein was used as a marker for paracellular transport. SFTI-1 was studied at two concentrations, 250 nM and 500 nM whereas kalata B1 was studied at five concentrations, 250, 500, 1000, 2000, and 4000 nM due to detection issues at lower concentrations.

In vitro binding assay

In order to determine the binding of both small molecular drugs and peptides to plasma proteins and brain tissue homogenate, as well as the binding of

peptides to lung tissue homogenate and cell lysate, equilibrium dialysis was performed. These experiments allow us to measure the parameters unbound fraction in plasma ($f_{u,plasma}$) and unbound fraction in tissue ($f_{u,tissue}$) in plasma and diluted tissue homogenate from brains or lungs. In these experiments PBS was spiked with the studied compound and added to one side of the semipermeable membrane, with the biological matrix being studied on the other side of the membrane. The membrane in these studies had a molecular weight cut off of 12-13 kDa allowing for both small molecules and peptides to cross through, whilst restricting the passage of proteins and tissue components. The device used for the equilibrium dialysis was in a high-throughput 96 well format, allowing for measurement of the unbound fraction in different matrices at the same time, with multiple replicates. The experiment was run for 6 h at 37 °C in a MaxQ4450 shaker (Thermo Fisher Scientific, NinoLab, Sweden) at 200 rpm. The interaction between the studied compound and the binding sites in plasma or tissue are generally assumed to be reversible and an assumption is that equilibrium is rapidly reached between the bound and unbound fractions. This allows measuring the unbound fraction as the ratio between the concentrations of the compound in the receiver side and the donor side at equilibrium. This was calculated as follows:

$$f_{u,plasma} = \frac{C_{buffer}}{C_{plasma}} \quad (\text{Eq 7})$$

For $f_{u,brain/lung}$ there was a need to compensate for the dilution of the homogenate, and the following equation was used:

$$f_{u,h,D} = \frac{C_{buffer}}{C_{homogenate}} \quad (\text{Eq 8})$$

$$f_{u,tissue} = \frac{\frac{1}{D}}{\left(\left(\frac{1}{f_{u,h,D}}\right) - 1\right) + \frac{1}{D}} \quad (\text{Eq 9})$$

In these equations $f_{u,h,D}$ is the diluted tissue homogenate, and D is the dilution factor [27]. The dilution factor used for brain and lung homogenate was 5, whereas the dilution of cell lysate in Paper IV was 35.3.

In vitro unbound tissue volume of distribution assay

The tissue slice method for measuring $V_{u,brain}$ was used in Papers I, III, and IV. The methods have been described in full in Fridén et al and Bäckström et al [30,64]. Here follows a brief summary of the methods. For the brain slices, six coronal slices were cut from the striatal area of drug naïve rats at a

thickness of 300 μm using a Leica VT1200 microtome slicer (Leica Microsystems, Wetzlar, Germany). These were incubated with 200 nM of the studied drug in 15 mL of artificial extracellular fluid (aECF) for 5 hours in a MaxQ4450 shaker incubator (Thermo Fischer Scientific, NinoLab, Sweden). After the incubation the slices were dried on filter paper, weighed, and homogenised in nine volumes (w/v) of aECF. The buffer was sampled directly from the dish in which the experiment was performed. $V_{u,brain}$ was then determined with the following equation.

$$V_{u,brain} = \frac{A_{slice} - V_i * C_{buffer}}{C_{buffer}(1 - V_i)} \quad (\text{Eq 10})$$

In this equation, A_{slice} stands for the measured concentration of compound in the slice per g tissue, C_{buffer} is the concentration in the buffer at the end of the experiment. V_i is the volume of buffer film coating the slice, which has been determined to a value of 0.094 mL/g brain [30].

In Paper IV, brain slice experiments were also run at 4°C to elucidate whether any active processes were involved in the uptake and distribution of the peptides (Figure 4). These experiments followed the same procedures as previously described. Experiments with blockers or modulators of uptake pathways were also run. In these experiments the slices were pre-incubated with monensin or dynasore for 30 min prior to the addition of either SFTI-1 or kalata B1. Monensin was chosen as an ionophore modulator of the pH in the subcellular compartments, decreasing the potential for lysosomal trapping. The chosen concentration of monensin was 50 nM which was the highest tolerable concentration in the slices, able to elicit an effect without compromising the viability of the slices [32,65,66]. Dynasore is a dynamin inhibitor which prevents the formation of clathrin and caveolin coated vesicles in the cell membrane [67,68]. The concentration used was 50 μM which was previously shown to provide a 70 % decrease in dynamin activity.

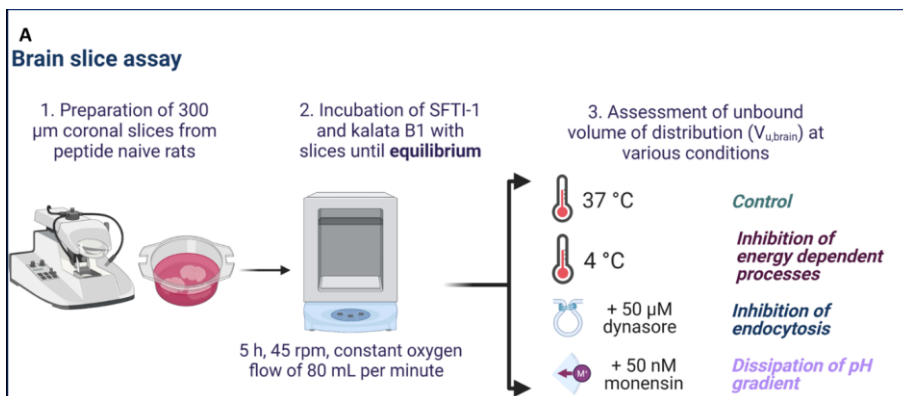


Figure 4. Experimental setup for brain slice assay. Illustration by Irena Loryan. Created with Biorender.

For the lung slice experiments an in situ perfusion of rat lungs was performed with physiological saline, after which the lungs were filled with agarose type VII-A to facilitate slicing. The slices were prepared with a Leica VT1200 microtome at a thickness of 500 μm . Three slices from three biological replicates were incubated in 15 mL of aECF for 5h with a peptide concentration of 200 nM. The slices were then sampled in the same way as the brain slices, with drying and sampling of the buffer. $V_{u,\text{lung}}$ was calculated in the same way as $V_{u,\text{brain}}$, but with a different V_i value, 0.73 mL/g lung, since the liquid film layer surrounding lung slices differ from the one for brain slices.

Cellular accumulation assay

In order to assess the cellular accumulation of the cyclic peptides SFTI-1 and kalata B1, they were incubated with stem cell derived neurons and astrocytes differentiated from human neural stem cells (hNSCs) [69]. These cells were seeded at a density of 2.5×10^4 cells/ cm^2 in triplicates per cell type on six well plates. The peptides were added to Neurobasal medium to a concentration of 500 nM and 2 mL of this peptide containing medium was added to each well. The cells were incubated for 5 hours at 37°C with the peptides, after which the medium was removed and the cells were lysed with 300 μL of Pierce lysis buffer per well. Samples were later kept at -20°C pending analysis.

The uptake of the peptides into cells was calculated with the concentration ratio $K_{p,u,\text{cell}}$, which is the ratio of total cellular-to-unbound medium concentrations. This is a partition coefficient between unbound concentrations in the buffer and total concentrations in the cells, meaning that the partitioning coefficient is a composite of both the uptake in the cells, and the distribution driven by binding to cellular components. That means that this parameter is

similar in concept to $V_{u,brain}$, giving a description of uptake and binding characteristics. $K_{p,u,cell}$ is calculated using the following equation:

$$K_{p,u,cell} = \frac{C_{cell}}{C_{medium}} \quad (\text{Eq 11})$$

C_{cell} is the measured concentration in the lysed cells, calculated as the amount of peptide in the cell lysate divided by the volume of the cells in the lysate. The cell volume was determined through the measurement of protein content in the cell lysate. A volume of 6.5 $\mu\text{L}/\text{mg}$ protein was then used to determine the total cell volume [70]. C_{medium} is the measured concentration in the medium. $K_{p,u,cell}$ can further be used to calculate $K_{p,uu,cell}$ for the specific cell type by combining $K_{p,u,cell}$ with $f_{u,cell}$ measured with equilibrium dialysis.

$$K_{p,uu,cell} = K_{p,u,cell} * f_{u,cell} \quad (\text{Eq 12})$$

This $K_{p,uu,cell}$ value describe the cellular accumulation in specific cell types, in contrast to the $K_{p,uu,cell}$ determined from brain slice experiments where all cell types present in the brain are involved, and can therefore differ from values obtained from those experiments.

Bioanalytical setup

For the quantification of both the antipsychotic drugs and the peptides high quality LC-MS methods were used. In Paper I an LC-MS/MS setup was used, where the LC system was set up with two LC-10AD pumps coupled to a SIL-HTc autosampler (Shidmadzu, Kyoto, Japan). The separation was performed on a HyPurity C18 column (3 μm particle size, 50 x 4.6 mm, Thermo Scientific, Waltham, MA, USA). Quantification was carried out on a Quattro Ultima Pt (Waters, Milford, MA, USA) using multiple reaction monitoring in positive electrospray mode.

In Paper II, the analytical method for kalata B1 was developed. It was performed with LC-10AD pumps coupled to a SIL-HTc autosampler connected to the aforementioned HyPurity C18 column. Quantification was performed on the Quattro Ultima Pt. Validation was performed to determine the accuracy and precision of the method as well as the LLOQ and linear range. The validation was performed in accordance with the FDA guidance of validation of bioanalytical methods [71]. Intra- and inter-day accuracy and precision were determined by the analysis of all standards, as well as six replicates of each QC during one day. The LLOQ was determined by running five LLOQ-candidates at the same time as the standards and QC samples. The accuracy was described as the deviation of the measured concentration from the nominal concentration as a percentage. The precision was

determined with the coefficient of variation (CV) and was obtained by dividing the standard deviation with the mean concentration of the measured samples. The CV was below 15 % for all QC levels in both plasma and brain homogenate. The accuracy was also within the threshold of 15 % deviation from the nominal concentrations.

In Papers III and IV quantification of kalata B1 and SFTI-1 was performed on either a Quattro Ultima Pt or on a Xevo TQ-S micro triple quadrupole mass spectrometer (Waters, Milford, MA, USA). The LC system was either the LC-10AD pumps with a SIL-HTc autosampler or an Acquity UPLC (Waters, Milford, MA, USA). The columns were a HyPurity C18 and a Peptide CSH C18 (50 x 2.1 mm, particle size 1.7 μ m) (Waters, MA, USA). For Paper I, the LC separation was performed using a gradient based on two mobile phases, mobile phase A with 0.1 % formic acid in water, and mobile phase B with 90 % acetonitrile in water with 0.1 % formic acid. In Papers II-IV LC separation was performed with the following mobile phases, mobile phase A with 10 % acetonitrile in water with 0.5 % formic acid, and mobile phase B with 90 % acetonitrile in water with 0.5 % formic acid. The observed retention times for the two peptides were 1.85 min and 3.47 min for kalata B1 and SFTI-1 respectively, thereby enabling fast analysis of the peptide samples.

Results & Discussion

Regional distribution of antipsychotics (Paper I)

Paper I shows quantitative evidence of differences in BBB transport between different regions of the brain. It also shows regional differences in brain tissue binding.

The paper describes the neuropharmacokinetics of haloperidol, clozapine, olanzapine, quetiapine, risperidone, and paliperidone, including their regional BBB transport in the following regions of the CNS; frontal cortex, striatum, hippocampus, brainstem, cerebellum, hypothalamus, and the spinal cord. The paper also describes the regional intra-brain distribution and binding, with $f_{u,brain}$ and $V_{u,brain}$ being measured for all compounds in cortex, striatum, and coronal brain slices. With these parameters measured, using the combinatory mapping approach, we could spatially map the differences in transport and distribution for antipsychotic drugs in the CNS.

With the exception of clozapine which had a uniform BBB transport throughout all regions, all the compounds exhibited significant spatial differences in their BBB transport (Figure 5). The largest differences in BBB transport were seen for risperidone and paliperidone, which are both quite strong Pgp substrates. This could signify differences in expression levels of the efflux proteins, or differences in their functionality between sites. The studied antipsychotics were effluxed at the BBB with the exception of haloperidol and olanzapine with $K_{p,uu,brain}$ values ranging from 1.5 to 0.05 throughout the study. When looking at the different regions, cerebellum showed the most efficient efflux for all compounds, whereas cortex showed the least efficient efflux. An example of these differences was seen for risperidone, with a 5.4-fold difference in $K_{p,uu,brain}$ between frontal cortex (0.28 ± 0.11) and cerebellum (0.05 ± 0.02). Another clear example of the spatial differences was seen for paliperidone, with a 4-fold difference in $K_{p,uu,brain}$ between frontal cortex (0.12 ± 0.03) and the spinal cord (0.03 ± 0.009). These findings are clear proofs that assumptions of uniform distribution to the brain are not valid, and that the BBB characteristics vary between brain regions. This is therefore something that should be kept in mind when developing therapeutics with a target in a specific brain region, or side effects linked to another brain region than that of the target.

When looking at the brain tissue binding of the different antipsychotics, the binding capacity varied 24-fold between the lowest recorded $f_{u,brain}$ value, 0.007 for clozapine in spinal cord, and the highest $f_{u,brain}$ value of 0.17 paliperidone in hypothalamus. Olanzapine and paliperidone had similar binding in all regions, but the other studied compounds exhibited significant differences in binding between the different regions. When looking at the $V_{u,brain}$ values for the antipsychotics, studied in cortex and striatum, there was a clear trend towards higher binding and/or uptake in striatum compared to cortex for all compounds except for risperidone. By calculating the $K_{p,uu,cell}$ value for the antipsychotics in order to evaluate their intracellular accumulation, it was found that olanzapine, clozapine and paliperidone all accumulated in cells, with olanzapine having on average 5-fold higher intracellular concentrations compared to extracellular concentrations. As binding, both specific and non-specific, plays a significant role in the distribution of drugs, and we show that this binding, as well as cellular uptake can vary significantly between different regions of the brain, it is clearly not enough to measure total concentrations in the brain when assessing the potential of therapeutic agents targeting the CNS. Rather, by combining unbound, regional concentrations with the receptor occupancy needed to elicit an effect, it is possible to accurately predict the effect of a compound, as well as any side effect that may arise from the measured concentrations. In fact, these findings might be part of the explanation as to why newer atypical antipsychotics have not performed better than their older typical counterparts [72,73]. Another important lesson from this study is the fact that it is not only the $K_{p,uu,brain}$ value of a compound that determines its capability to function as an effective agent within the CNS, since we show that two of the studied antipsychotic agents have $K_{p,uu,brain}$ values below 0.2 indicating major efflux at the BBB. Rather, one must regard the extent of BBB transport in conjunction with the potency of the drug, and thereby establish a proper, site-of-action, PKPD-relationship in order to fully appreciate the potential of a given compound to elicit an effect within the CNS.

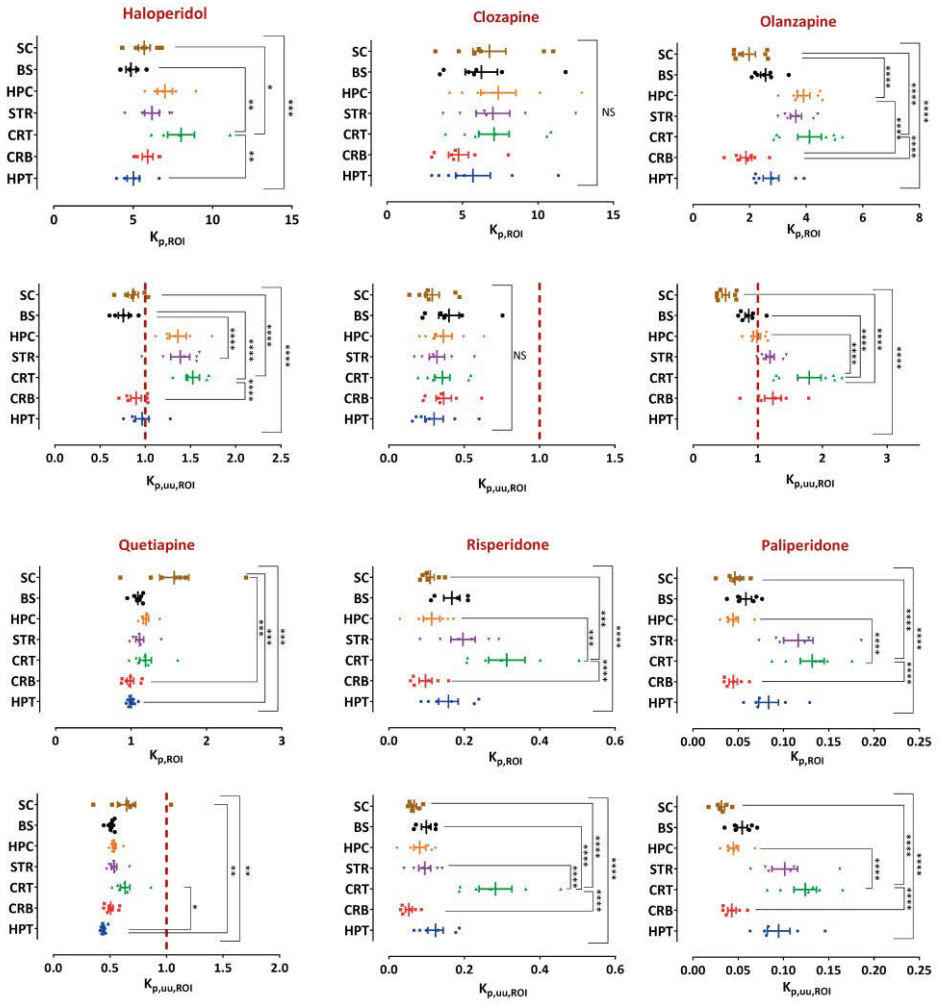


Figure 5. $K_{p,brain}$ and $K_{p,uu,brain}$ graphs for the six studied antipsychotics in the studied regions of the brain; spinal cord (SC), brain stem (BS), hippocampus (HPC), striatum (STR), cortex (CRT), cerebellum (CRB), hypothalamus (HPT). Individual values and averages. *) $p < 0.05$, **) $p < 0.01$, ***) $p < 0.001$, ****) $p < 0.0001$

Validation of bioanalytical method for kalata B1 (Paper II)

Paper II describes the validation of the bioanalytical method for kalata B1. This method was robust, simple, and with sufficient sensitivity for the quantification of kalata B1 in plasma and brain homogenate, matrices essential for the determination of BBB transport. The linear range in plasma was 2-10000 ng/mL and in brain tissue it was 5-2000 ng/mL. The LLOQs in plasma and brain homogenate were 2 ng/mL and 5 ng/mL respectively.

The inter- and intra-day precision and accuracy were assessed and were found to be low and within the acceptable limits. The precision had a CV < 15 % at both inter- and intra-day assessment, and the accuracy was within ± 12 %, both for the inter- and intra-day validation. These levels of accuracy and precision were found in both plasma and brain homogenate and provided a clear starting point for analysis of biological samples of the cyclic peptide. The method was applied to assess the systemic pharmacokinetics of kalata B1, describing the half-life of the peptide. When developing the method it was noticed that interfering peaks appeared. It was found that a fragment of human keratin has the same mass as the studied ion of kalata B1. This issue was resolved by preparing the samples in a clean environment. Another issue discovered in the method development was the sticking of kalata B1 to glassware. This resulted in high variability in sample concentrations. This issue was remediated through silanization of the glassware, which eliminated the sticking issue, as well as using low binding plastic tubes for sample preparation.

Blood-brain barrier transport of cyclic peptides (Paper III)

Paper III describes the BBB transport of two cyclic peptides, the smaller SFTI-1, isolated from sunflower seeds, and the cyclotide kalata B1, isolated from the plant *oldenlandia affinis*. The paper describes the systemic pharmacokinetics of the peptides, as well as their in vivo extent of BBB transport and the in vitro permeability across an endothelial cell BBB model.

The results from the in vivo pharmacokinetics study confirm the in vivo stability of the cyclic peptides, with relatively long half-lives of 20-30 minutes for both peptides (Figure 6). Both of the peptides had relatively similar clearance (CL) values of 1.82 and 1.60 mL/min/kg for SFTI-1 and kalata B1, respectively. These values are close to the renal filtration rate of rats, which coupled with the high metabolic stability of the cyclic peptides indicate a primarily renal excretion of these peptides. The plasma protein binding of both peptides was also assessed, with SFTI-1 being highly unbound, whereas kalata B1 exhibiting a higher degree of plasma protein binding with $f_{u,plasma}$ values of 0.936 ± 0.038 and 0.299 ± 0.095 for SFTI-1 and kalata B1 respectively.

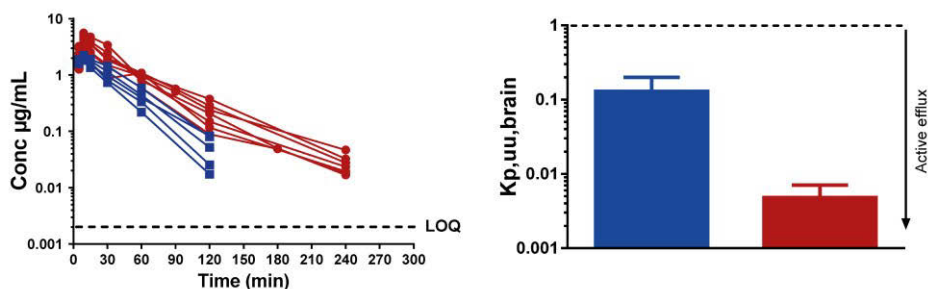


Figure 6. Plasma pharmacokinetics and BBB transport of SFTI-1 (blue) and kalata B1 (red).

In vivo blood-brain barrier transport

The assessment of BBB transport of SFTI-1 and kalata B1 was performed with a constant rate infusion over four hours. $K_{p,brain}$ was calculated as the total concentration ratio between brain and plasma of the steady state concentrations at four hours. By combining the $K_{p,brain}$ values with $f_{u,plasma}$ and $V_{u,brain}$ the extent of BBB transport at equilibrium at steady state, $K_{p,uu,brain}$ was assessed and was found to be 0.129 ± 0.0698 for SFTI-1 and 0.00479 ± 0.00229 for kalata B1, indicating efflux or restricted entry across the BBB. Interestingly, SFTI-1 had a higher extent of BBB transport, more than 25 times that of kalata B1, despite earlier reports on the cell penetrating capabilities of kalata B1 [41,42].

The $V_{u,brain}$ values of the two peptides were also determined, with kalata B1 having a significantly higher $V_{u,brain}$ than SFTI-1, a sign of high intra-brain distribution, indicating high levels of binding to brain tissue, or cellular accumulation within the cells of the brain parenchyma. The cellular accumulation was calculated with the parameter $K_{p,uu,cell}$, where it was shown that SFTI-1 is restricted from entering the cells of the brain with a $K_{p,uu,cell}$ value of 0.415 ± 0.079 , whereas kalata B1 accumulates within the same cells with a $K_{p,uu,cell}$ of 9.73 ± 3.35 .

These results show a duality in the behaviour of the peptides, where SFTI-1 is able to penetrate the BBB to a much higher extent than kalata B1, but when studying the cellular accumulation within the brain tissue, the opposite is true, where kalata B1 is penetrating into the cells, whereas SFTI-1 is restricted to the interstitial fluid. The results in this study show the importance of performing experiments in the relevant tissue or cell type. These findings suggest that SFTI-1 could be a suitable candidate for further development as a BBB delivery system, provided the active moiety has a relatively high potency, as SFTI-1 is still kept out of the brain to a rather large extent.

Table 2. Systemic and brain distribution pharmacokinetic parameters (mean \pm SD) for SFTI-1 and kalata B1.

Parameter	Unit	SFTI-1	Kalata B1
Systemic parameters			
Area under the plasma drug concentration-time curve from time zero to infinity, $AUC_{0-\infty}$	$\mu\text{g} \cdot \text{min}/\text{mL}$	77.3 ± 17.2	168 ± 38.1
Half-life, $t_{1/2}$	min	20.3 ± 3.50	35.8 ± 3.52
Systemic clearance, CL	$\text{mL}/\text{min}/\text{kg}$	1.82 ± 0.48	1.60 ± 0.396
Apparent volume of distribution, V_d	mL/kg	191 ± 34.4	322 ± 88.7
Fraction of unbound in plasma, $f_{u, \text{plasma}}$	unitless	0.936 ± 0.038	0.299 ± 0.095
Brain distribution parameters			
Total brain-to-plasma concentration ratio, $K_{p, \text{brain}}$	unitless	0.0618 ± 0.0318	0.234 ± 0.083
Unbound brain-to-plasma concentration ratio, $K_{p, \text{uu}, \text{brain}}$	unitless	0.129 ± 0.0698	0.00479 ± 0.0023
Total steady-state plasma concentration, $C_{\text{plasma}, \text{ss}}$	nanomole/L	400 ± 46.9	1096 ± 149

In vitro blood-brain barrier permeability

To determine the rate of transport of the studied peptides, a set of experiments were performed to assess the permeability of the peptides across an in vitro BBB model. These studies showed a low permeability for both peptides with an average P_e value of 0.228×10^{-3} cm/min for SFTI-1 and an average of 0.230×10^{-3} cm/min for kalata B1, i.e. no significant different difference between the two peptides (Figure 7). The measured P_e values were also lower than the paracellular marker sodium fluorescein, and the cyclic peptide cyclosporine A [74]. No differences in permeability were seen between the studied concentrations of peptide, suggesting that there is no concentrations dependency within the studied concentration range. The fact that there was no significant difference in the permeability between the two peptides, reinforces the fact that the permeability of a compound is not directly linked to its extent of BBB transport at equilibrium. It was also found that a fraction of the administered amount of kalata B1 accumulated within the endothelial cell layer, rather than penetrate through it. This gives some support to the reported cell penetrating capability of kalata B1, but should also be seen as part of the complexity of the assessment of CPPs, since kalata B1 is able to penetrate into the endothelial cells, but not cross through cell layer.

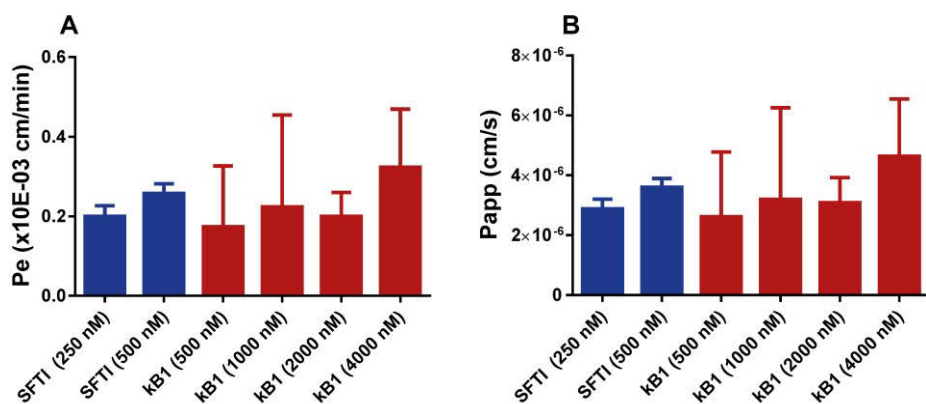


Figure 7. BBB permeability of SFTI-1 (blue) and kalata B1 (red) assessed in a human in vitro BBB model. No differences were found between the concentration levels. All data are presented as mean \pm SD.

The findings in this study expands on previous work of the cell penetrating capabilities of SFTI-1 and kalata B1, but adds valuable insight in this behaviour in vivo, as well as the properties of the BBB regarding their transport. Since all previous studies, have been performed either in cell cultures of peripheral cell types such as HeLa cells or MCF-7 cells, or in synthetic membranes based on phosphatidylcholine, adding the barrier properties of

the BBB and studying the process in vivo provides knowledge on the capabilities of CPPs as carriers targeting the CNS [41,42,61,62].

Intra-brain distribution and cellular uptake of cyclic peptides (Paper IV)

Paper IV describes the intra-brain distribution and cellular uptake into neurons and astrocytes, as well as compares the tissue uptake in brain with that in lung tissue. Since it was observed in Paper III that SFTI-1 was able to penetrate the BBB but not the cells of the brain parenchyma, whilst the opposite was true for kalata B1, it became evident that further studies were needed on this phenomenon, and in particular the intra-brain distribution of these two peptides. The first step here was to investigate whether any active processes were involved in the overall distributions of the peptides in brain slices, and therefore brain slice experiments were carried out at 4° C. For SFTI-1, no change in $V_{u,brain}$ was observed with a $V_{u,brain}$ of 0.436 ± 0.0665 mL/g brain at 37° C and 0.503 ± 0.148 mL/g brain at 4° C, not surprising considering its limited distribution at 37° C (Figure 8). For kalata B1 on the other hand, a huge decrease was observed when performing the experiments under cold conditions with the $V_{u,brain}$ falling from 152 ± 30.9 to 1.13 ± 0.253 mL/g brain, almost entirely negating any distribution of the peptide in the brain tissue. When calculating the $K_{p,uu,cell}$ values this further reinforced the earlier results, indicating that kalata B1 does indeed undergo some form of active accumulation into the cells of the brain, as the $K_{p,uu,cell}$ dropped from 9.73 ± 3.35 to below 1 when going from 37° C to 4° C, where a $K_{p,uu,cell} > 1$ indicates active uptake or accumulation and a value < 1 indicates that there are processes that restricts the cellular entry of the peptide.

To further elucidate the distribution pathways of SFTI-1 and kalata B1 in the brain, two different experiments were performed. First, in order to assess to what extent pH partitioning governs the intra-brain distribution, brain slice experiments were performed with a 30 min pre-incubation with the ionophore monensin. This pre-incubation caused significant, but rather small 30 % reductions in $V_{u,brain}$ and $K_{p,uu,cell}$ of both peptides, suggesting some influence of the pH gradient in the distribution of the peptides. Perhaps a more important process in the distribution of larger molecules is endocytosis. The effect of dynamin dependent endocytosis was assessed by pre-incubation with the dynamin inhibitor dynasore for 30 min. Dynasore pre-incubation did not affect the distribution of SFTI-1, but caused a 23 % decrease in $V_{u,brain}$ and $K_{p,uu,cell}$ of kalata B1.

In order to investigate whether the high distribution and accumulation of kalata B1 in brain was tissue dependent or a general process, lung slice ex-

periments were performed. These experiments showed rather surprising results, with no accumulation observed at all for kalata B1 in lung tissue. This value obtained from lung tissue slices is almost exactly the same as the one obtained from the brain slice experiments performed at 4°C. This suggests that the distribution of kalata B1 is tissue dependent, and could be brain specific.

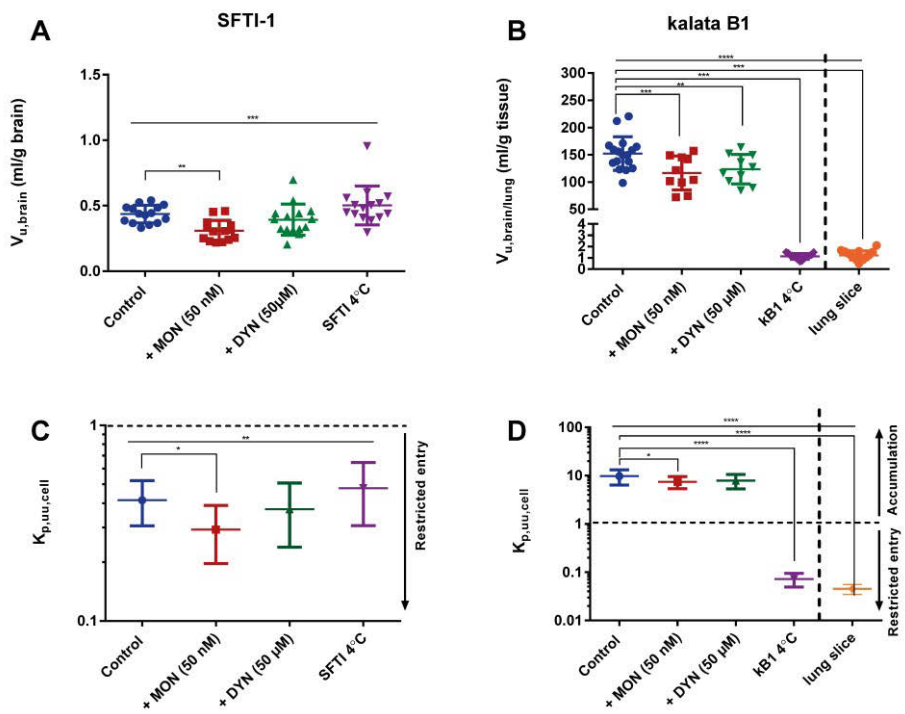


Figure 8. Intra-brain distribution of SFTI-1 and kalata B1. A, B: $V_{u,brain}$ of SFTI-1 and kalata B1 with a comparison between a control group and slices pre-incubated with monensin or dynasore, as well as experiments performed at 4°C. C, D: $K_{p,u,u,cell}$ results for SFTI-1 and kalata B1. Individual slice data in A & D, and mean values \pm SD in C & D.

Cellular uptake of SFTI-1 and kalata B1

To further investigate the cellular accumulation of the cyclic peptides, their uptake was studied in separate cell cultures of neurons and astrocytes. These cells were differentiated from human neuronal stem cells. The trend of the results was the same as in previous experiments, with SFTI-1 exhibiting lower accumulation than kalata B1. The main difference between the cellular accumulation experiments and those performed in brain slices was that SFTI-1 showed signs of accumulation in the cell cultures, compared to in brain slices where no accumulation was observed. It was also observed that

the accumulation tended to be higher in neurons compared to astrocytes. When calculating $K_{p,uu,cell}$ values from the cellular uptake study, it was noted that these values differed from those obtained from the slice experiments, in that SFTI-1 exhibited higher intracellular accumulation, 10.7 and 5.80 in neurons and astrocytes respectively, compared to kalata B1 with $K_{p,uu,cell}$ values of 2.08 and 3.08 in neurons and astrocytes. This might be an effect of the high binding to the cell lysate that was observed, with potential differences in binding sites available when comparing cells derived from human stem cells to rat brain slices, but could also be driven by differences between how cells behave in isolation compared to whole tissue. Further studies would be needed to fully understand this phenomenon.

Conclusions

This thesis describes a thorough framework for the assessment and evaluation of regional BBB transport and intra-brain distribution, with insights from *in vivo* and *in vitro* methodologies. The use of these combined methods allows for the estimation of unbound, active concentration with high spatial specificity. As many drug targets within the CNS are either differentially expressed within the brain, or are located intracellularly within different cell types of the brain, knowledge of the distribution of drugs within the CNS is crucial. This thesis shows the need for specific and detailed methodology to assess both BBB penetration and intra-brain distribution, and the importance of combining the two.

In particular, this thesis shows the concrete existence of regional differences in the extent of BBB transport of antipsychotics, as well as their intracellular distribution and binding to brain components. These findings contribute to the understanding of how the effect/side-effect profile of antipsychotics work, and shows that the differences in BBB transport between regions of the brain contribute to differential receptor occupancy of risperidone and olanzapine in particular.

In order to properly evaluate the distribution of compounds within the CNS, sensitive, quantitative analytical methods are required. To that end, it was crucial to develop a LC-MS/MS method for the quantitative analysis of cyclic peptides in both plasma and brain homogenate. In Paper II, such a method was developed and validated. The method had good precision and accuracy as well as high specificity for kalata B1. The method was successfully applied to *in vivo* samples of kalata B1, showing promise for further studies of the peptide in biological matrices. The approach taken in this study also aided in the development of a method for SFTI-1.

In Papers III and IV the BBB transport and intra-brain distribution was determined both *in vivo* and *in vitro*. The BBB transport of SFTI-1 and kalata B1 showed clear differences. SFTI-1 was able to penetrate the BBB to a relatively high extent for a peptide, indicating that it might be useable as a scaffold for delivery to the CNS. Kalata B1 on the other hand was unable to penetrate the BBB to any meaningful extent, despite previous reports of cell penetrating capabilities. This reinforces the understanding of the BBB as an extremely protective and specific barrier. Another finding from these studies is that the restrictive nature of the BBB was also captured by the *in vitro*

BBB model based on human brain endothelial cells. To be noted is that the permeability of the peptides were very similar, again showing that the rate and extent of BBB are different processes and that measuring one does not necessarily inform about the properties of the other. It was identified that the cellular accumulation of kalata B1 could be negated by performing the experiments under cold conditions, suggesting active processes, and that both pH gradients and dynamin dependent processes contributed to the accumulation of kalata B1. SFTI-1 on the other exhibited no penetration into cells when studied in tissue studies. When the accumulation was studied in cell cultures of neurons and astrocytes, it was however observed that both peptides tended to accumulate, indicating a difference between cultured cells and ex vivo tissue.

In conclusion this thesis and the studies herein contribute to a better understanding of distribution patterns of both antipsychotics and cyclic peptides and provides valuable lessons in terms of what types of studies should be prioritized for the development of such molecules into therapeutic agents, laying a groundwork for future studies on spatial and cellular distribution studies within the CNS.

Acknowledgements

The work presented in this thesis was performed at the Department of Pharmacy, Faculty of Pharmacy in collaboration with the Department of Pharmaceutical Biosciences, Faculty of Pharmacy, both at Uppsala University. I would like to thank the Swedish Research Council (Vetenskapsrådet) for their funding that contributed to this project (grant no. 2011-4339). I am also thankful of Apotekarsocieteten and Anna-Maria Lundins stiftelse at Smålands Nation for their generous travel grants that allowed me to attend and present at international conferences.

I would like to express my deep gratitude to all the people who have in one way or another been a part of this thesis, in particular:

My main supervisor Margareta Hammarlund-Udenaes for accepting me as a PhD student in your lab, for all your support when times were tough, for your outstanding scientific vision, and for all discussions we've had, about science, but also about organizations, society, and everything in-between.

My co-supervisor Irena Loryan for jumping into the project when it was already started, but taking it on with all your enthusiasm and energy. Thank you for all your support during the finishing stretch of this journey.

My co-supervisor Ulf Göransson for always being positive about the project, for providing me with the peptides, and for giving a different perspective on what I'm doing. Thank you for encouraging me to travel to Australia and present my work, and for providing insight into the world of cyclic peptides.

My collaborators at Uppsala University: Camilla Eriksson, Robert Fredriksson, Kimia Hosseini, thank you for giving me your expertise and time. With your contributions this project got new insights and perspectives.

My collaborators at the Laboratoire de la Barrière Hémato-Encéphalique, Université d'Artois, Lens, France; Maxime Culot and Sara Wellens. Our collaboration was extremely fruitful, thank you for making sure I understood the data that was produced, and providing crucial knowledge.

Jessica Dunhall, thank you so much for all your help in the lab. For always being supportive, and for always trying again when things didn't work out.

Britt Jansson, thank you for trusting me in the lab when I was completely new. For teaching me so much about LC-MS, and for being part of the second paper.

Former colleagues in the tPKPD group: Sofia and Annika, you were the best mentors I could have hoped for when I started in the group. Thank you for all the little tips and trick to help me settle in. Nebojsa, for being an awesome friend, colleague, and travel companion. Thank you for all the fun we had, both in the lab and around the world.

Yang, we started in the lab at around the same time, and now we're leaving around the same time. Thank you for all the good discussions, about science, food, and the world.

Frida, thank you for bringing new energy to the lab, and for making these last couple of years extra fun.

Jörgen, thank you for giving me the chance to test my wings as a lecturer, and for being incredibly supportive. The students don't know how lucky they are to have you. All the other teachers at the division for Pharmacokinetics & Pharmacotherapy, for your help with all my teaching assignments, for being good and kind colleagues.

Annelie, Caroline, Ilse, and Rebecka, who would have thought that organizing a conference, would lead to such good friends. Thank you for all the memes, chats, and fun times.

All friends from the Pharmacometrics group, for making the department a genuinely nice place; it was (almost) always fun to go to work.

Adam and Lukas, my good friends outside of BMC, for proving some much needed reality checks, and fun times in Stockholm and Köpenhamn/Malmö.

My parents and family, for always providing an exceptional support network and always believing in me.

Erik Melander
Uppsala December 2021

References

- [1] Abbott NJ, Patabendige AAK, Dolman DEM, Yusof SR, Begley DJ. Structure and function of the blood–brain barrier. *Neurobiol Dis* 2010;37:13–25. <https://doi.org/10.1016/j.nbd.2009.07.030>.
- [2] Abbott NJ. Blood-brain barrier structure and function and the challenges for CNS drug delivery. *J Inher Metab Dis* 2013;36:437–49. <https://doi.org/10.1007/s10545-013-9608-0>.
- [3] Begley DJ, Brightman MW. Structural and functional aspects of the blood-brain barrier. *Prog Drug Res Fortschritte Arzneimittelforschung Progres Rech Pharm* 2003;61:39–78. https://doi.org/10.1007/978-3-0348-8049-7_2.
- [4] Wolburg H, Noell S, Mack A, Wolburg-Buchholz K, Fallier-Becker P. Brain endothelial cells and the glio-vascular complex. *Cell Tissue Res* 2009;335:75–96. <https://doi.org/10.1007/s00441-008-0658-9>.
- [5] Wolburg H, Lippoldt A. Tight junctions of the blood-brain barrier: development, composition and regulation. *Vascul Pharmacol* 2002;38:323–37.
- [6] Pardridge WM. Drug and gene delivery to the brain: the vascular route. *Neuron* 2002;36:555–8. [https://doi.org/10.1016/s0896-6273\(02\)01054-1](https://doi.org/10.1016/s0896-6273(02)01054-1).
- [7] Bradbury MW, Stubbs J, Hughes IE, Parker P. THE DISTRIBUTION OF POTASSIUM, SODIUM, CHLORIDE AND UREA BETWEEN LUMBAR CEREBROSPINAL FLUID AND BLOOD SERUM IN HUMAN SUBJECTS. *Clin Sci* 1963;25:97–105.
- [8] Abbott NJ, Rönnbäck L, Hansson E. Astrocyte-endothelial interactions at the blood-brain barrier. *Nat Rev Neurosci* 2006;7:41–53. <https://doi.org/10.1038/nrn1824>.
- [9] Bernacki J, Dobrowolska A, Nierwińska K, Małecki A. Physiology and pharmacological role of the blood-brain barrier. *Pharmacol Rep PR* 2008;60:600–22.
- [10] Nadal A, Fuentes E, Pastor J, McNaughton PA. Plasma albumin is a potent trigger of calcium signals and DNA synthesis in astrocytes. *Proc Natl Acad Sci U S A* 1995;92:1426–30.
- [11] Gingrich MB, Traynelis SF. Serine proteases and brain damage - is there a link? *Trends Neurosci* 2000;23:399–407. [https://doi.org/10.1016/s0166-2236\(00\)01617-9](https://doi.org/10.1016/s0166-2236(00)01617-9).
- [12] Gingrich MB, Junge CE, Lyuboslavsky P, Traynelis SF. Potentiation of NMDA receptor function by the serine protease thrombin. *J Neurosci Off J Soc Neurosci* 2000;20:4582–95.
- [13] Scholz M, Cinatl J, Schädel-Höpfner M, Windolf J. Neutrophils and the blood-brain barrier dysfunction after trauma. *Med Res Rev* 2007;27:401–16. <https://doi.org/10.1002/med.20064>.

- [14] Cserr HF, Cooper DN, Suri PK, Patlak CS. Efflux of radiolabeled polyethylene glycols and albumin from rat brain. *Am J Physiol* 1981;240:F319-328. <https://doi.org/10.1152/ajprenal.1981.240.4.F319>.
- [15] Brown PD, Davies SL, Speake T, Millar ID. Molecular mechanisms of cerebrospinal fluid production. *Neuroscience* 2004;129:957–70. <https://doi.org/10.1016/j.neuroscience.2004.07.003>.
- [16] Meltzer HY. Update on typical and atypical antipsychotic drugs. *Annu Rev Med* 2013;64:393–406. <https://doi.org/10.1146/annurev-med-050911-161504>.
- [17] Kapur S, Langlois X, Vinken P, Megens AAHP, De Coster R, Andrews JS. The differential effects of atypical antipsychotics on prolactin elevation are explained by their differential blood-brain disposition: a pharmacological analysis in rats. *J Pharmacol Exp Ther* 2002;302:1129–34. <https://doi.org/10.1124/jpet.102.035303>.
- [18] Hammarlund-Udenaes M, Fridén M, Syvänen S, Gupta A. On the rate and extent of drug delivery to the brain. *Pharm Res* 2008;25:1737–50. <https://doi.org/10.1007/s11095-007-9502-2>.
- [19] Uchida Y, Ohtsuki S, Katsukura Y, Ikeda C, Suzuki T, Kamiie J, et al. Quantitative targeted absolute proteomics of human blood-brain barrier transporters and receptors. *J Neurochem* 2011;117:333–45. <https://doi.org/10.1111/j.1471-4159.2011.07208.x>.
- [20] Dagenais C, Rousselle C, Pollack GM, Scherrmann JM. Development of an in situ mouse brain perfusion model and its application to *mdr1a* P-glycoprotein-deficient mice. *J Cereb Blood Flow Metab Off J Int Soc Cereb Blood Flow Metab* 2000;20:381–6. <https://doi.org/10.1097/00004647-200002000-00020>.
- [21] Vandenhoute E, Dehouck L, Boucau M-C, Sevin E, Uzbekov R, Tardivel M, et al. Modelling the neurovascular unit and the blood-brain barrier with the unique function of pericytes. *Curr Neurovasc Res* 2011;8:258–69. <https://doi.org/10.2174/156720211798121016>.
- [22] Cecchelli R, Aday S, Sevin E, Almeida C, Culot M, Dehouck L, et al. A stable and reproducible human blood-brain barrier model derived from hematopoietic stem cells. *PloS One* 2014;9:e99733. <https://doi.org/10.1371/journal.pone.0099733>.
- [23] Takasato Y, Rapoport SI, Smith QR. An in situ brain perfusion technique to study cerebrovascular transport in the rat. *Am J Physiol* 1984;247:H484-493. <https://doi.org/10.1152/ajpheart.1984.247.3.H484>.
- [24] Hellinger E, Veszelka S, Tóth AE, Walter F, Kittel A, Bakk ML, et al. Comparison of brain capillary endothelial cell-based and epithelial (MDCK-MDR1, Caco-2, and VB-Caco-2) cell-based surrogate blood-brain barrier penetration models. *Eur J Pharm Biopharm Off J Arbeitsgemeinschaft Pharm Verfahrenstechnik EV* 2012;82:340–51. <https://doi.org/10.1016/j.ejpb.2012.07.020>.
- [25] Gupta A, Chatelain P, Massingham R, Jonsson EN, Hammarlund-Udenaes M. Brain distribution of cetirizine enantiomers: comparison of three different tissue-to-plasma partition coefficients: $K(p)$, $K(p,u)$, and $K(p,uu)$. *Drug Metab Dispos Biol Fate Chem* 2006;34:318–23. <https://doi.org/10.1124/dmd.105.007211>.

- [26] Koch-Weser J, Sellers EM. Binding of drugs to serum albumin (first of two parts). *N Engl J Med* 1976;294:311–6. <https://doi.org/10.1056/NEJM197602052940605>.
- [27] Kalvass JC, Maurer TS. Influence of nonspecific brain and plasma binding on CNS exposure: implications for rational drug discovery. *Biopharm Drug Dispos* 2002;23:327–38. <https://doi.org/10.1002/bdd.325>.
- [28] Loryan I, Sinha V, Mackie C, Van Peer A, Drinkenburg W, Vermeulen A, et al. Mechanistic understanding of brain drug disposition to optimize the selection of potential neurotherapeutics in drug discovery. *Pharm Res* 2014;31:2203–19. <https://doi.org/10.1007/s11095-014-1319-1>.
- [29] Di L, Umland JP, Chang G, Huang Y, Lin Z, Scott DO, et al. Species independence in brain tissue binding using brain homogenates. *Drug Metab Dispos Biol Fate Chem* 2011;39:1270–7. <https://doi.org/10.1124/dmd.111.038778>.
- [30] Fridén M, Ducrozet F, Middleton B, Antonsson M, Bredberg U, Hammarlund-Udenaes M. Development of a high-throughput brain slice method for studying drug distribution in the central nervous system. *Drug Metab Dispos Biol Fate Chem* 2009;37:1226–33. <https://doi.org/10.1124/dmd.108.026377>.
- [31] Loryan I, Fridén M, Hammarlund-Udenaes M. The brain slice method for studying drug distribution in the CNS. *Fluids Barriers CNS* 2013;10:6. <https://doi.org/10.1186/2045-8118-10-6>.
- [32] Fridén M, Bergström F, Wan H, Rehngren M, Ahlin G, Hammarlund-Udenaes M, et al. Measurement of unbound drug exposure in brain: modeling of pH partitioning explains diverging results between the brain slice and brain homogenate methods. *Drug Metab Dispos Biol Fate Chem* 2011;39:353–62. <https://doi.org/10.1124/dmd.110.035998>.
- [33] Andreone BJ, Chow BW, Tata A, Lacoste B, Ben-Zvi A, Bullock K, et al. Blood-Brain Barrier Permeability Is Regulated by Lipid Transport-Dependent Suppression of Caveolae-Mediated Transcytosis. *Neuron* 2017;94:581–594.e5. <https://doi.org/10.1016/j.neuron.2017.03.043>.
- [34] Razani B, Lisanti MP. Caveolins and caveolae: molecular and functional relationships. *Exp Cell Res* 2001;271:36–44. <https://doi.org/10.1006/excr.2001.5372>.
- [35] Xiao G, Gan L-S. Receptor-mediated endocytosis and brain delivery of therapeutic biologics. *Int J Cell Biol* 2013;2013:703545. <https://doi.org/10.1155/2013/703545>.
- [36] Niewoehner J, Bohrmann B, Collin L, Urich E, Sade H, Maier P, et al. Increased brain penetration and potency of a therapeutic antibody using a monovalent molecular shuttle. *Neuron* 2014;81:49–60. <https://doi.org/10.1016/j.neuron.2013.10.061>.
- [37] Manich G, Cabezón I, del Valle J, Duran-Vilaregut J, Camins A, Pallàs M, et al. Study of the transcytosis of an anti-transferrin receptor antibody with a Fab' cargo across the blood-brain barrier in mice. *Eur J Pharm Sci Off J Eur Fed Pharm Sci* 2013;49:556–64. <https://doi.org/10.1016/j.ejps.2013.05.027>.

- [38] Herce HD, Garcia AE, Litt J, Kane RS, Martin P, Enrique N, et al. Arginine-rich peptides destabilize the plasma membrane, consistent with a pore formation translocation mechanism of cell penetrating peptides. *Biophys J* 2009;97:1917–25. <https://doi.org/10.1016/j.bpj.2009.05.066>.
- [39] Copolovici DM, Langel K, Eriste E. *Cell-Penetrating Peptides: Design, Synthesis, and Applications* 2014;8:23.
- [40] Matsuzaki K, Yoneyama S, Murase O, Miyajima K. Transbilayer transport of ions and lipids coupled with mastoparan X translocation. *Biochemistry* 1996;35:8450–6. <https://doi.org/10.1021/bi960342a>.
- [41] Henriques ST, Huang Y-H, Chaousis S, Sani M-A, Poth AG, Separovic F, et al. The Prototypic Cyclotide Kalata B1 Has a Unique Mechanism of Entering Cells. *Chem Biol* 2015;22:1087–97. <https://doi.org/10.1016/j.chembiol.2015.07.012>.
- [42] Henriques ST, Huang Y-H, Rosengren KJ, Franquelim HG, Carvalho FA, Johnson A, et al. Decoding the membrane activity of the cyclotide kalata B1: the importance of phosphatidylethanolamine phospholipids and lipid organization on hemolytic and anti-HIV activities. *J Biol Chem* 2011;286:24231–41. <https://doi.org/10.1074/jbc.M111.253393>.
- [43] Frankel AD, Pabo CO. Cellular uptake of the tat protein from human immunodeficiency virus. *Cell* 1988;55:1189–93. [https://doi.org/10.1016/0092-8674\(88\)90263-2](https://doi.org/10.1016/0092-8674(88)90263-2).
- [44] Green M, Loewenstein PM. Autonomous functional domains of chemically synthesized human immunodeficiency virus tat trans-activator protein. *Cell* 1988;55:1179–88. [https://doi.org/10.1016/0092-8674\(88\)90262-0](https://doi.org/10.1016/0092-8674(88)90262-0).
- [45] Derossi D, Joliot AH, Chassaing G, Prochiantz A. The third helix of the Antennapedia homeodomain translocates through biological membranes. *J Biol Chem* 1994;269:10444–50.
- [46] Myrberg H, Zhang L, Mäe M, Langel U. Design of a tumor-homing cell-penetrating peptide. *Bioconjug Chem* 2008;19:70–5. <https://doi.org/10.1021/bc0701139>.
- [47] Mäe M, Langel U. Cell-penetrating peptides as vectors for peptide, protein and oligonucleotide delivery. *Curr Opin Pharmacol* 2006;6:509–14. <https://doi.org/10.1016/j.coph.2006.04.004>.
- [48] Fonseca SB, Pereira MP, Kelley SO. Recent advances in the use of cell-penetrating peptides for medical and biological applications. *Adv Drug Deliv Rev* 2009;61:953–64. <https://doi.org/10.1016/j.addr.2009.06.001>.
- [49] Deshayes S, Plénat T, Aldrian-Herrada G, Divita G, Le Grimellec C, Heitz F. Primary amphipathic cell-penetrating peptides: structural requirements and interactions with model membranes. *Biochemistry* 2004;43:7698–706. <https://doi.org/10.1021/bi049298m>.
- [50] Jones AT, Sayers EJ. Cell entry of cell penetrating peptides: tales of tails wagging dogs. *J Control Release Off J Control Release Soc* 2012;161:582–91. <https://doi.org/10.1016/j.jconrel.2012.04.003>.
- [51] Madani F, Lindberg S, Langel U, Futaki S, Gräslund A. Mechanisms of cellular uptake of cell-penetrating peptides. *J Biophys Hindawi Publ Corp Online* 2011;2011:414729. <https://doi.org/10.1155/2011/414729>.

- [52] Mueller J, Kretzschmar I, Volkmer R, Boisguerin P. Comparison of cellular uptake using 22 CPPs in 4 different cell lines. *Bioconjug Chem* 2008;19:2363–74. <https://doi.org/10.1021/bc800194e>.
- [53] Nakase I, Hirose H, Tanaka G, Tadokoro A, Kobayashi S, Takeuchi T, et al. Cell-surface accumulation of flock house virus-derived peptide leads to efficient internalization via macropinocytosis. *Mol Ther J Am Soc Gene Ther* 2009;17:1868–76. <https://doi.org/10.1038/mt.2009.192>.
- [54] Park SE, Sajid MI, Parang K, Tiwari RK. Cyclic Cell-Penetrating Peptides as Efficient Intracellular Drug Delivery Tools. *Mol Pharm* 2019;17.
- [55] Dougherty PG, Sahni A, Pei D. Understanding Cell Penetration of Cyclic Peptides. *Chem Rev* 2019;119:10241–87. <https://doi.org/10.1021/acs.chemrev.9b00008>.
- [56] Abdalla MA, McGaw LJ. Natural Cyclic Peptides as an Attractive Modality for Therapeutics: A Mini Review. *Mol Basel Switz* 2018;23:E2080. <https://doi.org/10.3390/molecules23082080>.
- [57] Craik DJ, Daly NL, Bond T, Waine C. Plant cyclotides: A unique family of cyclic and knotted proteins that defines the cyclic cystine knot structural motif. *J Mol Biol* 1999;294:1327–36. <https://doi.org/10.1006/jmbi.1999.3383>.
- [58] Craik DJ, Swedberg JE, Mylne JS, Cemazar M. Cyclotides as a basis for drug design. *Expert Opin Drug Discov* 2012;7:179–94. <https://doi.org/10.1517/17460441.2012.661554>.
- [59] Burman R, Gunasekera S, Strömstedt AA, Göransson U. Chemistry and biology of cyclotides: circular plant peptides outside the box. *J Nat Prod* 2014;77:724–36. <https://doi.org/10.1021/np401055j>.
- [60] Ackerman SE, Currier NV, Bergen JM, Cochran JR. Cystine-knot peptides: emerging tools for cancer imaging and therapy. *Expert Rev Proteomics* 2014;11:561–72. <https://doi.org/10.1586/14789450.2014.932251>.
- [61] Contreras J, Elnagar AYO, Hamm-Alvarez SF, Camarero JA. Cellular uptake of cyclotide MCoTI-I follows multiple endocytic pathways. *J Control Release Off J Control Release Soc* 2011;155:134–43. <https://doi.org/10.1016/j.jconrel.2011.08.030>.
- [62] D’Souza C, Henriques ST, Wang CK, Craik DJ. Structural parameters modulating the cellular uptake of disulfide-rich cyclic cell-penetrating peptides: MCoTI-II and SFTI-1. *Eur J Med Chem* 2014. <https://doi.org/10.1016/j.ejmech.2014.06.047>.
- [63] Plan MRR, Göransson U, Clark RJ, Daly NL, Colgrave ML, Craik DJ. The Cyclotide Fingerprint in *Oldenlandia affinis*: Elucidation of Chemically Modified, Linear and Novel Macrocyclic Peptides. *ChemBioChem* 2007;8:1001–11. <https://doi.org/10.1002/cbic.200700097>.
- [64] Bäckström E, Lundqvist A, Boger E, Svanberg P, Ewing P, Hammarlund-Udenaes M, et al. Development of a Novel Lung Slice Methodology for Profiling of Inhaled Compounds. *J Pharm Sci* 2016;105:838–45. <https://doi.org/10.1002/jps.24575>.
- [65] Lake JR, Van Dyke RW, Scharschmidt BF. Acidic vesicles in cultured rat hepatocytes. Identification and characterization of their relationship to lysosomes and other storage vesicles. *Gastroenterology* 1987;92:1251–61.

- [66] Siebert GA, Hung DY, Chang P, Roberts MS. Ion-trapping, microsomal binding, and unbound drug distribution in the hepatic retention of basic drugs. *J Pharmacol Exp Ther* 2004;308:228–35. <https://doi.org/10.1124/jpet.103.056770>.
- [67] Macia E, Ehrlich M, Massol R, Boucrot E, Brunner C, Kirchhausen T. Dynasore, a Cell-Permeable Inhibitor of Dynamin. *Dev Cell* 2006;10:839–50. <https://doi.org/10.1016/j.devcel.2006.04.002>.
- [68] András IE, Toborek M. HIV-1 stimulates nuclear entry of amyloid beta via dynamin dependent EEA1 and TGF- β /Smad signaling. *Exp Cell Res* 2014;323:66–76. <https://doi.org/10.1016/j.yexcr.2014.01.027>.
- [69] Hosseini K, Lekholm E, Ahemaiti A, Fredriksson R. Differentiation of Human Embryonic Stem Cells into Neuron, Cholinergic, and Glial Cells. *Stem Cells Int* 2020;2020:8827874. <https://doi.org/10.1155/2020/8827874>.
- [70] Gillen CM, Forbush B. Functional interaction of the K-Cl cotransporter (KCC1) with the Na-K-Cl cotransporter in HEK-293 cells. *Am J Physiol* 1999;276:C328–336. <https://doi.org/10.1152/ajpcell.1999.276.2.C328>.
- [71] FDA. Guidance for Industry: Bioanalytical Method Validation 2013.
- [72] Lewis S, Lieberman J. CATIE and CUtLASS: can we handle the truth? *Br J Psychiatry J Ment Sci* 2008;192:161–3. <https://doi.org/10.1192/bjp.bp.107.037218>.
- [73] Leucht S, Cipriani A, Spineli L, Mavridis D, Orey D, Richter F, et al. Comparative efficacy and tolerability of 15 antipsychotic drugs in schizophrenia: a multiple-treatments meta-analysis. *Lancet Lond Engl* 2013;382:951–62. [https://doi.org/10.1016/S0140-6736\(13\)60733-3](https://doi.org/10.1016/S0140-6736(13)60733-3).
- [74] Bellwon P, Culot M, Wilmes A, Schmidt T, Zurich MG, Schultz L, et al. Cyclosporine A kinetics in brain cell cultures and its potential of crossing the blood-brain barrier. *Toxicol Vitro Int J Publ Assoc BIBRA* 2015;30:166–75. <https://doi.org/10.1016/j.tiv.2015.01.003>.

Acta Universitatis Upsaliensis

*Digital Comprehensive Summaries of Uppsala Dissertations
from the Faculty of Pharmacy 304*

Editor: The Dean of the Faculty of Pharmacy

A doctoral dissertation from the Faculty of Pharmacy, Uppsala University, is usually a summary of a number of papers. A few copies of the complete dissertation are kept at major Swedish research libraries, while the summary alone is distributed internationally through the series Digital Comprehensive Summaries of Uppsala Dissertations from the Faculty of Pharmacy. (Prior to January, 2005, the series was published under the title "Comprehensive Summaries of Uppsala Dissertations from the Faculty of Pharmacy".)

